Nanoporous Films

DOI: 10.1002/anie.200803071

Nanostructured TiO_2 Films Templated by Amphiphilic Dendritic Core–Double-Shell Macromolecules: From Isolated Nanorings to Continuous 2D Mesoporous Networks**

*Meizhen Yin, Yajun Cheng, Miaoyin Liu, Jochen S. Gutmann, and Klaus Müllen**

Crystalline TiO_2 with a controlled morphology has tremendous applications in many different fields such as photocatalysis, gas sensors, lithium-ion batteries, and dye-sensitized solar cells.[1] The working mechanisms of these functional materials are dominated by interfacial processes. Consequently, the performance of these materials is significantly influenced by their morphology.[2] Numerous reports have described the synthesis of nanoscale titania materials with different morphologies,[3] where small surfactant molecules or amphiphilic block copolymers were typically used as templating agents[3a–c,4] coupled with sol–gel chemistry. However, conventional block polymer micelles represent thermodynamic aggregates of amphiphilic molecules above their critical micelle concentration. Thus, block copolymer micelles are dynamically stable and their characteristics for a given system depend on the thermodynamic properties of the solvent and on temperature. The shape of the micellar structure might change upon varying the conditions, such as solvent, temperature, concentration, or pH. In contrast to these conventional micellar systems, dendritic core–shell macromolecules form "unimolecular micelles" in which the hydrophilic and hydrophobic segments are covalently connected with the dendritic core.[5] Therefore, their micellar structure is static rather than dynamic, which offers monodisperse and structurally stable spherical macromolecules.[6]

Herein, we report the design and use of a novel class of dendritic amphiphilic core–double-shell macromolecules (**P1a** and **P1b**, Scheme 1) as templates for the fabrication of well-organized, nanoporous thin TiO_2 films. The macromolecules consist of a central rigid polyphenylene dendrimer core and a flexible amphiphilic double-polymer shell with twelve arms, in which a polystyrene (PS) block serves as the hydrophobic segment and poly(acrylic acid) (PA) forms the hydrophilic moiety. The shape-persistent second-generation polyphenylene dendrimer core was selected as a scaffold as it

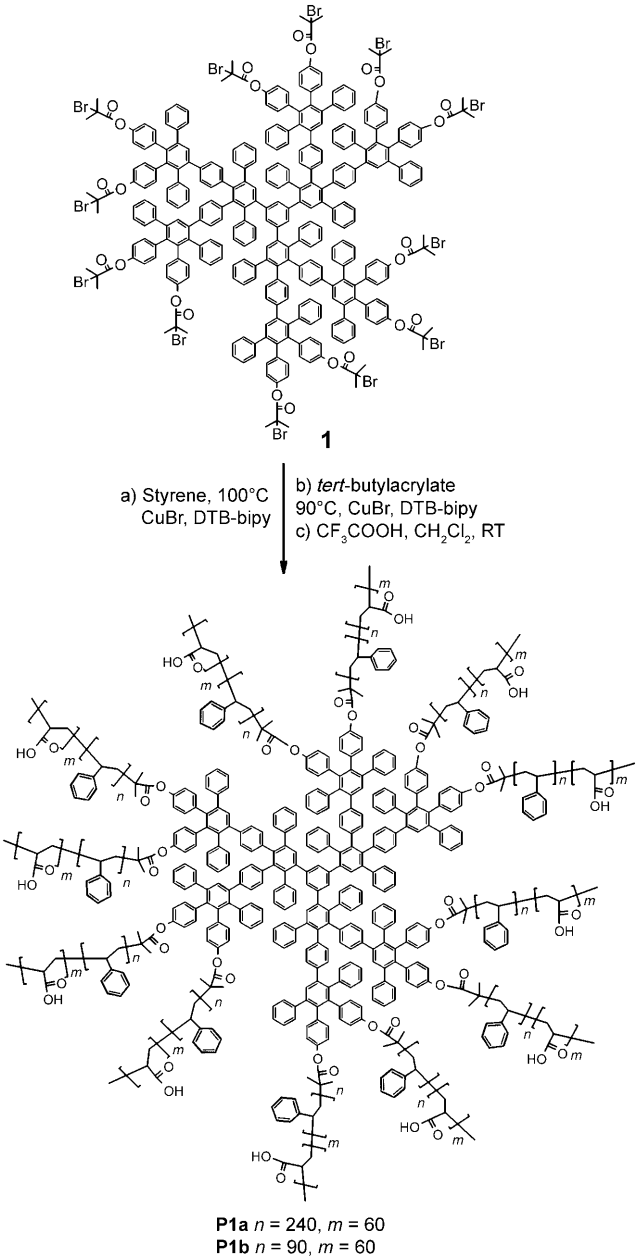

Scheme 1. Synthesis of dendritic amphiphilic core–double-shell macromolecules **P1a** and **P1b**. a) styrene, CuBr, 4,4′-di-*tert*-butyl-2,2′-bipyridine (DTB-bipy), 100 °C. b) *tert*-butyl acrylate, CuBr, DTB-bipy, 100 °C. c) CF_3COOH, CH_2Cl_2, RT.

[*] Dr. M. Yin, Dr. Y. Cheng,[+] M. Liu, Prof. J. S. Gutmann, Prof. K. Müllen
Max Planck Institute for Polymer Research
Ackermannweg 10, 55128 Mainz (Germany)
Fax: (+49) 6131-379-350
E-mail: muellen@mpip-mainz.mpg.de
Prof. J. S. Gutmann
Institute of Physical Chemistry, University of Mainz
Welderweg 11, Mainz (Germany)
[+] Current address: National Institute of Standards and Technology, 100 Bureau Drive, Gaithersburg, MD 20899 (USA)

[**] We thank G. Glasser for SEM studies and D. Cho for reading the manuscript. This work is financially supported by the Deutsche Forschungsgemeinschaft (SFB 625).
Supporting information for this article is available on the WWW under http://dx.doi.org/10.1002/anie.200803071.

provides a globular shape, a perfectly branched structure, and the availability of a defined number of functional groups at the surface that can undergo a further "grafting-from" procedure. The target of our research was the reproducible formation of TiO_2 thin films with specific morphologies by the systematic adjustment of the length of hydrophobic PS blocks in these dendritic amphiphilic core–double-shell macromolecules.

Scheme 1 shows the synthesis of dendritic amphiphilic core–double-shell macromolecules **P1a** and **P1b**, starting from the previously described macroinitiator **1**,[7a] which bears twelve 2-bromo-2-methylpropionic ester groups. Atom transfer radical polymerization (ATRP)[8] with styrene and further extension with *tert*-butyl acrylate was performed in a controlled manner, that is, as a controlled conversion below 20% in order to avoid intermolecular reactions. Subsequent removal of the *tert*-butyl protecting groups was achieved under acidic conditions to yield **P1a** and **P1b**. For comparison, a core–single-shell macromolecule **P2** (see below), which bears only *tert*-butyl acrylate as a monomer was

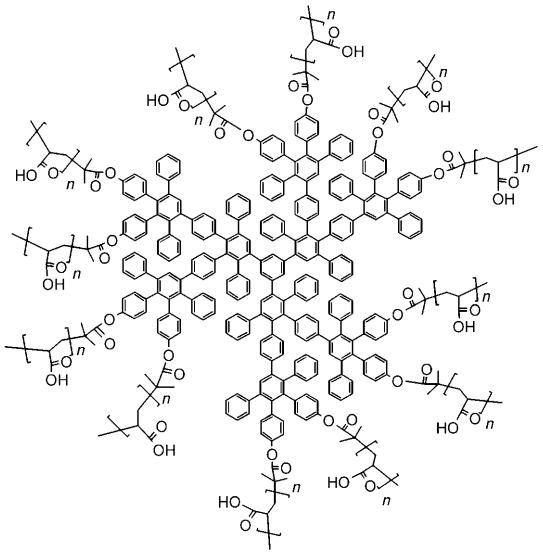

synthesized in a similar fashion. A detailed description of the synthetic procedure and the essential characterization of **P1a** and **P1b** and **P2** with FTIR and ^{1}H NMR spectroscopy are given in Schemes S1–S4, and Figures S1 and S2 in the Supporting Information.

Core-shell star polymers containing multiple arms connected to a central core have different properties compared to their linear analogues because of their compact structure and branched architecture. In accordance with previous experiments,[7] it was assumed that all twelve initiator sites were able to initiate the ATRP polymerization. The block lengths of the PS or PA polymer chains are given as repeating units (r.u.). The abbreviation PS(240)-b-PA(60) corresponds to 240 r.u. of polystyrene as a first polymer shell and 60 r.u. of PA as a secondary shell. One important characteristic of the core–shell system is the size of the particles, which is usually defined as the hydrodynamic radius (R_h) in a particular solvent. The R_h values of the synthesized core–shell particles were measured by dynamic light scattering (DLS) in DMF. The DLS data are summarized in Table 1. In case of **P1a** and

Table 1: DLS data of the amphiphilic core–double-shell star polymers (**P1a** and **P1b**) and the core–single-shell macromolecule (**P2**) in DMF ($L_{PS} = R_{hm} - R_{hc}$, $L_{PA} = R_{hd} - R_{hm}$).

No.	polymer	core, R_{hc} [nm]	core–single-shell, R_{hm} [nm]	L_{PS} [nm]	core-double-shell, R_{hd} [nm]	L_{PA} [nm]
P1a	PS(240)-b-PA(60)	1.5 ± 0.1	11.2 ± 0.2	9.7	14.6 ± 0.3	3.4
P1b	PS(90)-b-PA(60)	1.5 ± 0.1	5.8 ± 0.2	4.3	9.3 ± 0.2	3.5
P2	PA(100)	1.5 ± 0.1	6.6 ± 0.1	–	–	5.1[a]

[a] For **P2**, $L_{PA} = R_{hm} - R_{hc}$.

P1b, the block length of PS polymer chain was expressed by the difference of the hydrodynamic radii of the core–single-shell (R_{hm}) and that of dendrimer core (R_{hc}), that is, $L_{PS} = R_{hm} - R_{hc}$. Similarly, the block length of PA was calculated from the difference of the hydrodynamic radii of the core–double shell (R_{hd}) and R_{hm}, that is, $L_{PA} = R_{hd} - R_{hm}$. Table 1 shows that the particle size increases with polymer chain length, which is consistent with supplementary experiments.

We assumed that the core–double-shell template directs the formation of a micellar structure with a functional inorganic Ti–O– section in the outer shell (Scheme 2). This

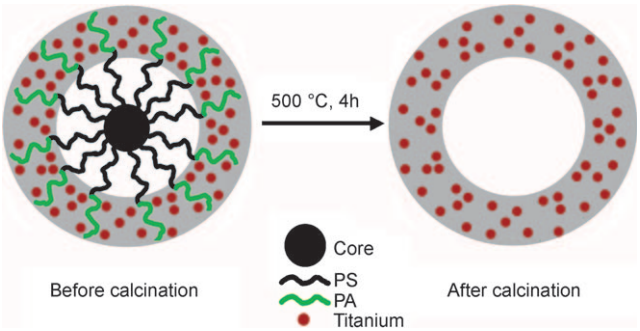

Scheme 2. Schematic illustration of the TiO_2 cyclization process templated by amphiphilic core–double-shell macromolecules.

occurs as titanium tetraisopropoxide (TTIP) can be incorporated into the outer PA shell through coordination bonds, but not into the inner PS shell. Subsequent hydrolysis and condensation of TTIP leads to the formation of covalent Ti–O– bonds between adjacent PA domains in one micelle. The complex solution is deposited onto a silicon wafer by spin coating. The organic section is removed by calcination, while the inorganic part forms a hollow TiO_2 shell or, if collapse occurs, a TiO_2 ring. The latter is more desirable in the fabrication of mesoporous films and may serve as a container for dyes in solar-cell applications. The size of the pore can therefore be controlled by the length of the hydrophobic PS block. We therefore proposed that the desired pore size of the

nanostructured TiO_2 could be obtained by systematically adjusting the length of hydrophobic PS block in the core–double-shell template.

To test this hypothesis, **P1a** was first used as a template to dictate the morphology of crystalline TiO_2. The morphology of crystalline TiO_2 was revealed by scanning electron microscopy (SEM) and atomic force microscopy (AFM). As expected, at a low concentration (1.25 mg mL^{-1} in DMF) and before calcination, the **P1a** complexes were distributed as isolated spherical structures on the surface of the silicon wafer (Figure 1A, C). The average radius of the sphere was (17 ± 1.5) nm, obtained from the AFM image (Figure 1A), and (16.5 ± 1.5) nm, calculated from the SEM image (Figure 1C). Although the radii of the **P1a** macromolecules were slightly larger than the R_{hd} value measured by DLS in solution (Table 1, $R_{hd} = 14.6$ nm), the height of the sphere calculated from the AFM image was significantly smaller ((15 ± 1) nm, Figure 1A) than the diameter of the core–shell template **P1a** in solution ($2 \times R_{hd} = 29.2$ nm). The decreased height and the increased diameter of the micelles were attributed to the partial flattening of the flexible polymer shells on the substrate during spin coating. After calcination, the isolated TiO_2 nanospheres were transformed into a ringlike structures with the same pore size (Figure 1B, D). The transformation in morphology indicates a collapse during calcination. The collapsed apical shell could overlay on the sidewall of the ring, because the sidewall of the ring was thicker than the theoretical value and the height of the ring was much lower than that of the TiO_2 nanosphere. AFM and SEM data showed that the thickness of the ring wall was (6 ± 1.2) nm, while the theoretical value is 3.4 nm. AFM height images showed the height of the TiO_2 ring to be (2.0 ± 0.2) nm, which was significantly smaller than the height of the sphere ((15 ± 1) nm)) before calcination. Both SEM and AFM measurements showed that the average pore radius was (12 ± 1) nm, which is consistent with the hydrophobic R_{hm} value of inner shell and core ($R_{hm} = 11.2$ nm in DMF, Table 1). These results therefore demonstrate that the initial hypothesis is valid and an amphiphilic core–double-shell macromolecule **P1a** successfully serves as a template to control the morphology of crystalline TiO_2.

Interestingly, many nanorings became connected to each other when the concentration of **P1a** was increased (2.5 mg mL^{-1} in DMF; Figure 1E and Figure S3 in the Supporting Information). This implies that the spherical micelles fuse together statically in solution if the concentration is high enough. As we considered the fusion between micelles to be advantageous, we increased the concentration of **P1a** to 5 mg mL^{-1} in DMF, which resulted in the formation of an organized continuous nanoporous TiO_2 film (Figure 1F and Figure S4 in the Supporting Information). X-ray reflectivity measurements showed the average film thickness to be 5.3 nm (Figure S5 in the Supporting Information). The pore size of the film was consistent with that of isolated TiO_2 nanorings. In general, we followed synthetic procedures common for conventional block copolymer templates—films from the complex solution were prepared after stirring for one hour.[3d] To show that the dendrimer micelles are more "robust", the **P1a** complex solution was stored for 20 days under argon at room temperature before spin coating. The morphology of the TiO_2 films from this solution was the same as that of the films obtained from fresh solutions. This demonstrated that **P1a** had a higher stability compared to conventional block copolymers because of to its special structure, and thus confirms the existence of its static stable micellar structure rather than a limited dynamic stable micellar system.

To control the pore size of the TiO_2 porous films, a strategy based on adjusting the hydrophobic block length was

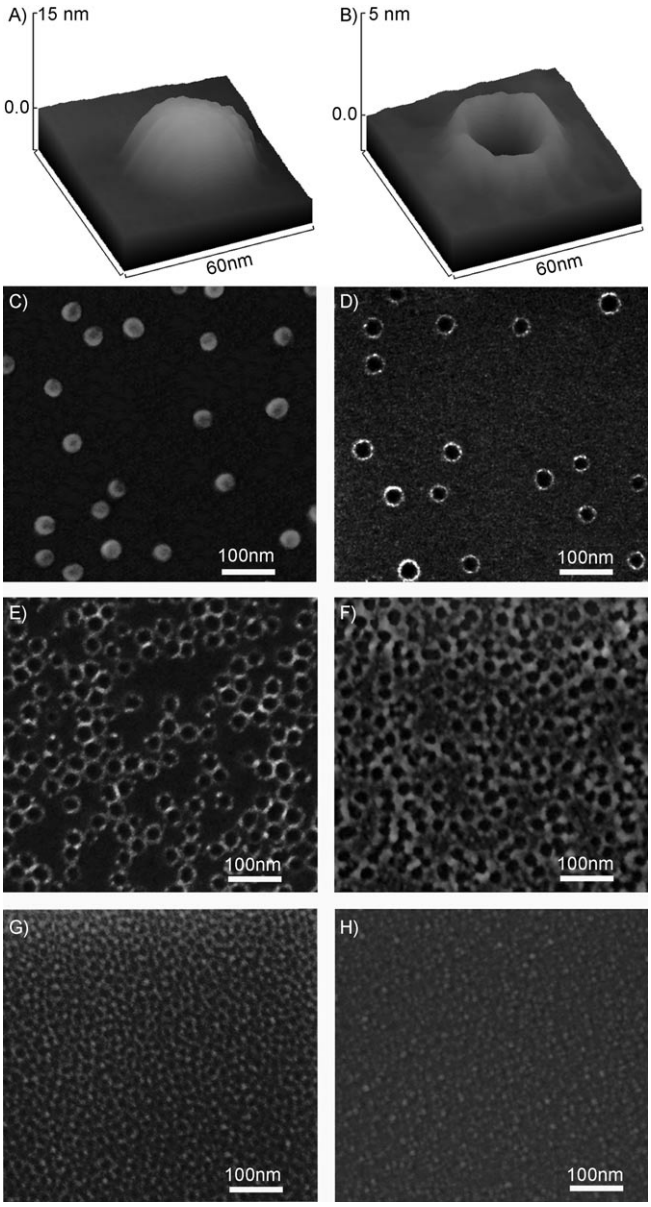

Figure 1. Dendritic amphiphilic core–double-shell macromolecules serve as templates to direct the morphogenesis of crystal TiO_2. Plot surface of AFM image of TiO_2 templated by **P1a** A) before and B) after calcination. SEM image of TiO_2 templated by C) **P1a** (1.0 mg mL^{-1}) in DMF before calcination; D) **P1a** (1.0 mg mL^{-1}) in DMF after calcination; E) **P1a** (2.5 mg mL^{-1}) in DMF after calcination; F) **P1a** (5.0 mg mL^{-1}) in DMF after calcination; G) **P1b** (5.0 mg mL$^{-1)}$ in DMF after calcination; H) **P2** (5.0 mg mL^{-1}) in DMF after calcination.

developed. Macromolecule **P1b**, which contains a hydrophilic segment of the same length but a shorter hydrophobic PS block ($R_{hm} = 5.8$ nm) than that of **P1a**, was designed as a template to tune the pore size. As expected, an organized continuous nanoporous TiO_2 film with a smaller pore (radius = (6 ± 1) nm, Figure 1G and Figure S6 in the Supporting Information) was achieved. The radius of the pore was in agreement with the R_{hm} values measured using DLS in solution ($R_{hm} = 5.8$ nm, Table 1). Therefore, the pore size of the film can be tuned by systematically varying the length of the hydrophobic block, which has further confirmed the process presented in Scheme 2.

To further investigate the templating effect of each shell on the porous TiO_2 film, a control templating agent, **P2**, bearing only a single shell of hydrophilic PA chains was synthesized. Compound **P2** was used to template the TiO_2 film in the same way as the double-shell macromolecule, this procedure resulted in a TiO_2 film without pore organization (Figure 1H and Figure S7 in the Supporting Information). This result indicates that the flexible hydrophobic PS shell is critical in the formation of organized porous TiO_2 films.

In summary, novel dendritic amphiphilic core–double-shell macromolecules were designed and applied as templates to tune the morphology of TiO_2 films. An isolated, well-defined TiO_2 nanoring was obtained with the template of a single amphiphilic core–double-shell molecule. At an appropriate complex concentration, these rings fused to form an organized nanoporous TiO_2 film. The pore size could be controlled by adjusting the length of the hydrophobic block in the inner shell of core–double-shell macromolecules. Thus, a new design of template molecules for controlling the morphogenesis of functional metal oxide films is available. The controllable pore size offers opportunities for potential applications, such as the penetration of hole conductor molecules in solar cells which require pore diameters larger than 10 nm. Future work on the application of the porous TiO_2 films in solar cells is in progress.

Experimental Section

Core-shell macromolecules (5, 10, or 20 mg) were dissolved in DMF (4.0 g) at room temperature, followed by the addition of the appropriate amounts of HCl (37%, 40 mg) solution and titanium tetraisopropoxide (TTIP, Aldrich, 97%, 35 mg) within 3 min and the solution was stirred for 1 h. Films were prepared on silicon wafer substrates by spin coating for 60.0 s using a Süss MicroTec Delta 80 spin coater under ambient conditions (rotation speed of 2000 rpm). The film thickness was measured by X-ray reflectivity using a Seifert diffractometer equipped with a mirror optic. The reflectivity curves were analyzed using Parratt32 software (Helmholtz-Zentrum Berlin).

Calcination of the films was carried out at 500 °C for 4 h in air at a heating rate of 6.25 °C min^{-1} starting from room temperature. After calcination, the samples were cooled to room temperature in the furnace.

Scanning electron microscopy (SEM) images were obtained on a field emission scanning electron microscope (LEO 1530 "Gemini"). The accelerating voltage was 1 kV. Atomic force microscopy (AFM) images were recorded using a Digital Instruments Dimension 3100 scanning force microscope in tapping mode equipped with Olympus cantilevers. The plot surface of AFM images were obtained using the ImageJ program.

Received: June 26, 2008
Published online: October 2, 2008

Keywords: amphiphiles · carboxylic acids · dendrimers · nanostructures · polymerization

[1] a) R. Wang et al., *Nature* **1997**, 388, 431–432; b) B. O'Regan, M. Grätzel, *Nature* **1991**, *353*, 737–740; c) A. Heller, *Acc. Chem. Res.* **1995**, *28*, 503–508; d) A. L. Linsebigler, G. Q. Lu, J. T. Yates, *Chem. Rev.* **1995**, *95*, 735–758; e) H. J. Snaith, L. Schmidt-Mende, *Adv. Mater.* **2007**, *19*, 3187–3200; f) L. Schmidt-Mende, J. E. Kroeze, J. R. Durrant, Md. K. Nazeeruddin, M. Grätzel, *Nano Lett.* **2005**, *5*, 1315–1320; g) L. Schmidt-Mende, M. Grätzel, *Thin Solid Films* **2006**, *500*, 296–301.

[2] a) Z. S. Wang, H. Kawauchi, T. Kashima, H. Arakawa, *Coord. Chem. Rev.* **2004**, *248*, 1381–1389; b) L. B. Roberson, L. A. Poggi, J. Kowalik, G. P. Smestand, L. A. Bottomley, L. M. Tolbert, *Coord. Chem. Rev.* **2004**, *248*, 1491–1499; c) C. Sanchez, C. Boissière, D. Grosso, C. Laberty, L. Nicole, *Chem. Mater.* **2008**, *20*, 682–737; d) P. Yang, M. Yang, S. Zou, J. Xie, W. Yang, *J. Am. Chem. Soc.* **2007**, *129*, 1541–1552.

[3] a) P. D. Cozzoli, A. Kornowski, H. Weller, *J. Am. Chem. Soc.* **2003**, *125*, 14539–14548; b) S. Y. Choi, M. Mamak, S. Speakman, N. Chopra, G. A. Ozin, *Small* **2005**, *1*, 226–232; c) Y. Cheng, J. S. Gutmann, *J. Am. Chem. Soc.* **2006**, *128*, 4658–4674; d) N. Satoh, T. Nakashima, K. Kamikura, K. Yamamoto, *Nat. Nanotechnol.* **2008**, *3*, 106–111; e) F. Caruso, R. A. Caruso, H. Möhwald, *Science* **1998**, *282*, 1111–1113; f) J. Lee, M. C. Orilall, S. C. Warren, M. Kamperman, F. J. Disalvo, U. Wiesner, *Nat. Mater.* **2008**, *7*, 222–228; g) A. Di Gianni, S. Trabelsi, G. Rizza, M. Sangermano, H. Althues, S. Kaskel, B. Voit, *Macromol. Chem. Phys.* **2007**, *208*, 76–86.

[4] a) H. M. Luo, C. Wang, Y. S. Yan, *Chem. Mater.* **2003**, *15*, 3841–3846; b) J. Lin, Y. Lin, P. Liu, M. J. Meziani, L. F. Allard, Y. P. Sun, *J. Am. Chem. Soc.* **2002**, *124*, 11514–11518; c) Y. Cheng, P. Müller-Buschbaum, J. S. Gutmann, *Small* **2007**, *3*, 1379–1382; d) S. Förster, V. Abetz, A. H. E. Müller, *Adv. Polym. Sci.* **2004**, *166*, 173–210; e) S. Förster, *Top. Curr. Chem.* **2003**, *226*, 1–28; f) D. H. Kim, S. H. Kim, K. Lavery, T. P. Russell, *Nano Lett.* **2004**, *4*, 1841–1844.

[5] M. Liu, K. Kono, J. M. J. Fréchet, *J. Controlled Release* **2000**, *65*, 121–131.

[6] a) A. W. Bosman, H. M. Janssen, E. W. Meijer, *Chem. Rev.* **1999**, *99*, 1665–1688; b) U. M. Wiesler, T. Weil, K. Müllen, *Top. Curr. Chem.* **2001**, *212*, 1–40; c) S. E. Stiriba, H. Frey, R. Haag, *Angew. Chem.* **2002**, *114*, 1385–1390; *Angew. Chem. Int. Ed.* **2002**, *41*, 1329–1334; d) P. Veprek, J. Jezek, *J. Pept. Sci.* **1999**, *5*, 203–220.

[7] a) M. Yin, R. Bauer, M. Klapper, K. Müllen, *Macromol. Chem. Phys.* **2007**, *208*, 1646–1656; b) M. Yin, J. Shen, G. O. Pflugfelder, K. Müllen, *J. Am. Chem. Soc.* **2008**, *130*, 7806–7807; c) M. Yin, J. Shen, R. Gropeanu, G. O. Pflugfelder, T. Weil, K. Müllen, *Small* **2008**, *4*, 894–898; d) M. Yin, K. Sorokina, C. Kuhlmann, C. Li, G. Mihov, K. Koynov, H. Luhmann, M. Klapper, K. Müllen, T. Weil, *Biomacromolecules* **2008**, *9*, 1381–1389.

[8] K. Matyjaszewski, J. Xia, *Chem. Rev.* **2001**, *101*, 2921–2990.

